Two CONSTANS-like 16 Genes

Subjects: Agriculture, Dairy & Animal Science

Contributor: Xinhua He

CONSTANS (CO) is an important regulator of photoperiodic flowering and functions at a key position in the flowering regulatory network. Here, two *CO* homologs, *MiCOL16A* and *MiCOL16B*, were isolated from “SiJiMi” mango to elucidate the mechanisms controlling mango flowering. The *MiCOL16A* and *MiCOL16B* genes were highly expressed in the leaves and expressed at low levels in the buds and flowers. The expression levels of *MiCOL16A* and *MiCOL16B* increased during the flowering induction period but decreased during the flower organ development and flowering periods.

mango CONSTANS flowering functional analysis

1. Introduction

In higher plants, floral transition is the process that describes the switch from the vegetative stage to the reproductive stage. The time for this process is referred to as flowering time. The flowering mechanism of the annual plant species *Arabidopsis* is thoroughly understood. According to recent research, the onset of flowering is regulated in a timely manner by an intricate network involving a series of regulatory pathways, such as gibberellin, photoperiod, autonomous, aging and vernalization pathways [1][2][3]. Of the many regulatory pathways, the photoperiod pathway is especially important; it is involved in plant responses to photoperiod sensing and subsequent molecular events [4].

Many photoperiod pathway-related genes have been discovered, such as TIME OF CAB EXPRESSION 1 (TOC1), LATE ELONGATED HYPOCOTYL (LHY), EARLY FLOWERING 4 (ELF4), GIGANTEA (GI), CIRCADIAN CLOCK ASSOCIATED 1 (CCA1), FLOWERING LOCUS T (FT) and CONSTANS (CO) [5]. Among them, CO is a key component of which there are orthologs in various plant species [6][7][8][9]. Currently, CYCLING DOF FACTOR (CDF) is known as the only transcription factor that directly binds to the CO promoter and suppresses the expression of CO [10][11][12]. The GI gene plays a key role in the photoperiod induction pathway and positively regulates the expression of the CO gene under long-day conditions [13]. Overexpression of the FLOWERING BHLH (FBH) gene elevates CO levels without being affected by photoperiod [14]. In addition, phytochrome-interacting factors (PIFs) interact with CO to suppress flowering [15]. The E3 ubiquitin ligase-encoding gene HIGH EXPRESSION OF OSMOTICALLY RESPONSIVE GENES1 (HOS1) is involved in controlling the abundance of CO, and CONSTITUTIVE PHOTOMORPHOGENIC1 (COP1), as a flowering repressor, is regulated by cryptochromes (CRY) and promotes the proteolysis of CO in the dark [16][17]. CO genes belong to the BBX family and can be divided into three categories according to their domains in Arabidopsis [7][18]. Group I genes have one

CO, CO-like, and TOC1 (CCT) domain and two B-box domains; group II genes have one B-box and one CCT domain; and group III genes have one B-box, one variant B-box and one CCT domain.

However, the functions of *CO* orthologs vary across different species. In *Arabidopsis*, overexpression of the *AtCO, AtCOL5* and *AtCOL16* genes promotes flowering under long-day (LD) or short-day (SD) conditions [19][20], but *AtCOL7, AtCOL8* and *AtCOL9* inhibit flowering under LD conditions [21][22]. In rice, the *OsHd1* gene delays flowering under LD conditions and promotes flowering under SD conditions [23], and *OsCOL16* inhibits flowering under both SD and LD conditions [24]. *StCO*, a *CO* homolog in potato, regulates flowering [25]. Moreover, the *CO* orthologs in Fuji apple, *MdCOL1* and *MdCOL2*, play a significant role in the growth and development of reproductive organs [26]. Thus, homologous *CO* genes have a wide range of effects on plant flowering and development.

Mango (*Mangifera indica* L.) is a member of the Anacardiaceae family and is an economically important fruit tree species. Flowering time has a considerable influence on the yield and quality of mango. Therefore, the discovery and identification of flowering-related genes are necessary for mango production. Mango flowering is the result of a complex process influenced by many factors, but it is not affected by daylength [27]. Several flowering-related regulatory genes have recently been identified in mango. For example, the *MiFT, MiSOC1* and *MiAP1* genes promote flowering, but the *MiCO* gene inhibits flowering in *Arabidopsis* [28][29][30][31]. However, the *COL16* gene has not been studied in mango.

2. Isolation and Analysis of MiCOL16A and MiCOL16B

Two *CO* homologs, *MiCOL16A* (GenBank No: MW326761) and *MiCOL16B* (GenBank No: MW326762), were identified from *M. indica.* L. cv. SiJiMi. The full cDNA sequences of *MiCOL16A* and *MiCOL16B* were 1269 bp and 1251 bp, encoding 423 and 417 amino acids, respectively; the two genes were 73.06% identical. The DNA sequences of *MiCOL16A* and *MiCOL16B* were 2030 bp and 1751 bp, respectively, and each contained one intron (**Figure 1**A). The alignment of *MiCOL16A* and *MiCOL16B* indicated that both have one CCT and one B-box domain and are highly conserved with other genes (**Figure 1**B). Phylogenetic analysis showed that these two genes were highly identical to *Arabidopsis* AtCOL6 and AtCOL16 in group II (**Figure 1**C). Therefore, these results indicated that *MiCOL16A* and *MiCOL16B* belong to group II genes of the *CO* gene family.

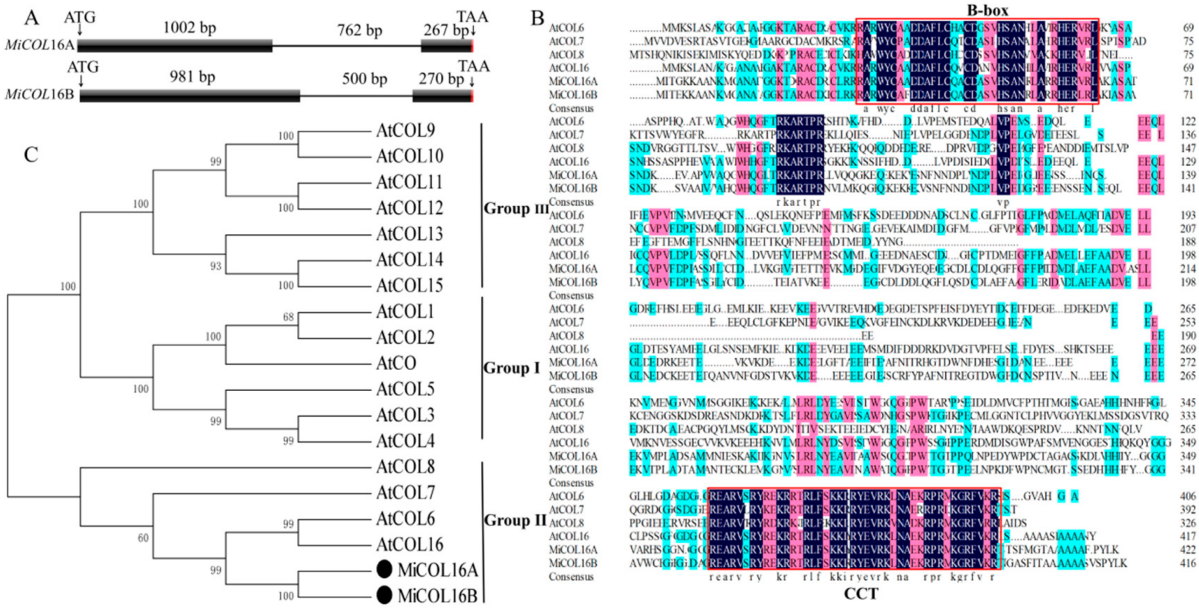

Figure 1. Sequence analysis of *MiCOL16A* and *MiCOL16B*. (**A**) Genomic structures of *MiCOL16A* and *MiCOL16B*. Exons are represented by black squares, and introns are represented by black lines. The numbers indicate the lengths of the corresponding regions. (**B**) Alignment of the predicted amino acid sequences of AtCOL6–8 and AtCOL16 in *Arabidopsis* and of MiCOL16A and MiCOL16B in mango. The conserved CCT and B-box domain regions are indicated with red boxes. The dark color indicates that the amino acids are 100% conserved. (**C**) Phylogenetic relationship of CO/COL proteins in *Arabidopsis* and mango. MiCOL16A and MiCOL16B are represented by black solid circles.

3. Expression of MiCOL16A and MiCOL16B in Mango

For the tissue-specific expression tests, qRT–PCR was performed. The results showed that *MiCOL16A* and *MiCOL16B* were expressed in all the tested tissues. On different branches, the expression levels of *MiCOL16A* and *MiCOL16B* in the leaves were always higher than those in the stems, buds or flowers, and the lowest expression levels of *MiCOL16A* and *MiCOL16B* were detected in the buds and flowers. In contrast, the expression level of *MiCOL16A* in the leaves of nonflowering branches was higher than that in the leaves of flowering branches (**Figure 2**A), but *MiCOL16B* expression was lower in the leaves of nonflowering branches than in those of flowering branches (**Figure 2**B).

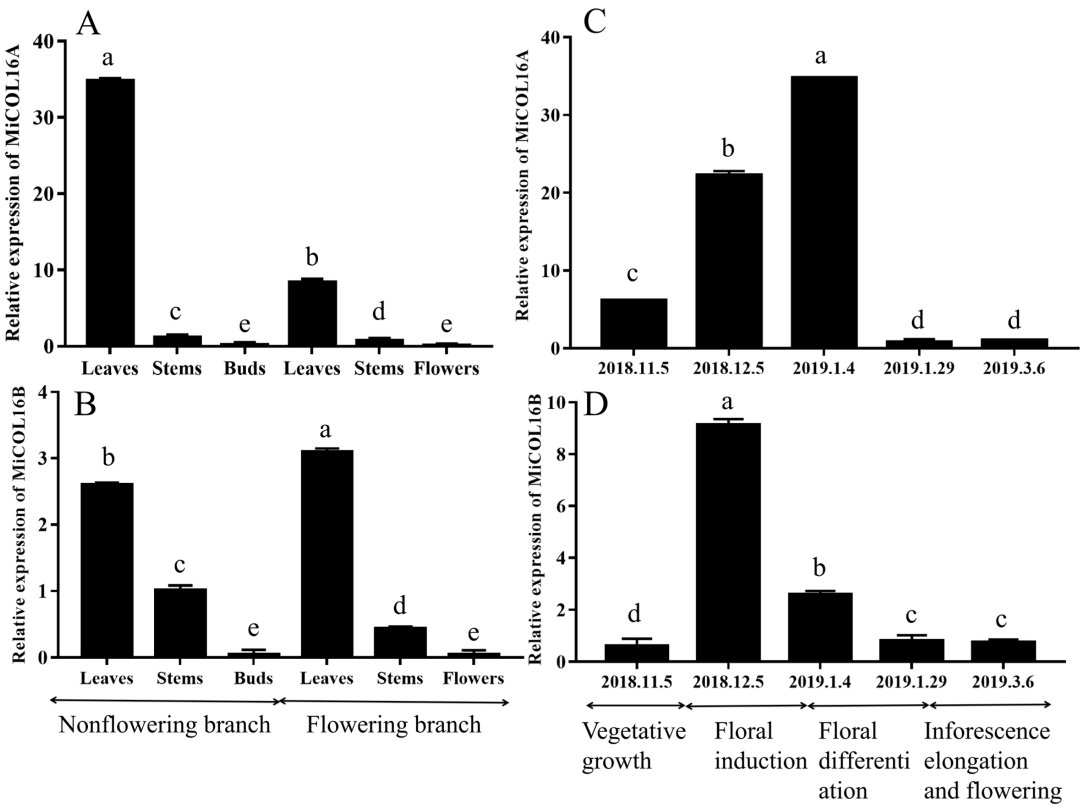

Figure 2. Tissue-specific and temporal expression analysis of the *MiCOL16A* and *MiCOL16B* genes. (**A**,**B**) Expression patterns of the *MiCOL16A* and *MiCOL16B* genes in different tissues of SiJiMi mango. (**C**,**D**) Expression patterns of the *MiCOL16A* and *MiCOL16B* genes at different time points.

To analyze the temporal expression patterns of *MiCOL16A* and *MiCOL16B*, qRT–PCR was performed. The results suggested that the two target genes were expressed in the leaves of mango at all tested periods. The expression pattern of *MiCOL16A* gradually increased from vegetative growth to the late floral induction period and then decreased (**Figure 2**C). However, *MiCOL16B* gene expression increased from the vegetative growth period to the early floral induction period and then decreased (**Figure 2**D).

The circadian-driven expression of *MiCOL16A* and *MiCOL16B* was determined using total RNA isolated from ‘SiJiMi’ mango leaves, which were collected every 3 h for three days. The results suggested that under LD conditions, the expression level of *MiCOL16A* started to increase after dusk, peaked 6 h after dusk and decreased rapidly thereafter before beginning to increase again after dusk (**Figure 3**A). Interestingly, this pattern also appeared under MD and SD conditions, and this result proved that *MiCOL16A* expression may be induced by night treatment and is not affected by the length of light (**Figure 3**C,E). The expression level of *MiCOL16B* fluctuated with time under different conditions, but there was no regularity. These results suggest that *MiCOL16A* expression exhibits a diurnal oscillation rhythm, but *MiCOL16B* expression is not affected by a diurnal rhythm (**Figure 3**B,D,F).

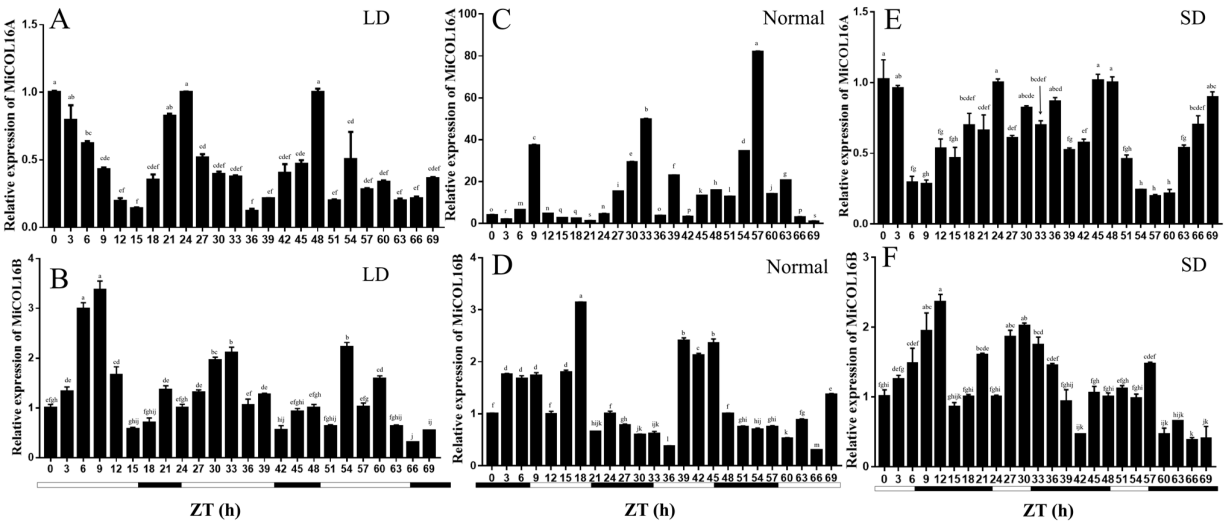

Figure 3. Expression analysis of the *MiCOL16A* and *MiCOL16B* genes in terms of circadian rhythm. (**A**,**C**,**E**) Expression patterns of *MiCOL16A* under LD (**A**), normal (**C**) and SD (**E**) conditions. (**B**,**D**,**F**) Expression patterns of *MiCOL16B* under LD (**B**), normal (**D**) and SD (**F**) conditions.

4. Both MiCOL16A and MiCOL16B Are Nuclear Proteins with Transcriptional Activation Activity

MiCOL16A and *MiCOL16B* protein-linked GFP fusion constructs driven by the CaMV 35S promoter were developed for molecular function assays. The GFP fusion constructs were inserted into vectors, which were transferred into onion inner epidermal cells. Single-strand analysis indicated that free GFP localized to the nucleus and cytomembrane, and both the MiCOL16A and MiCOL16B proteins localized to the nucleus (**Figure 4**A).

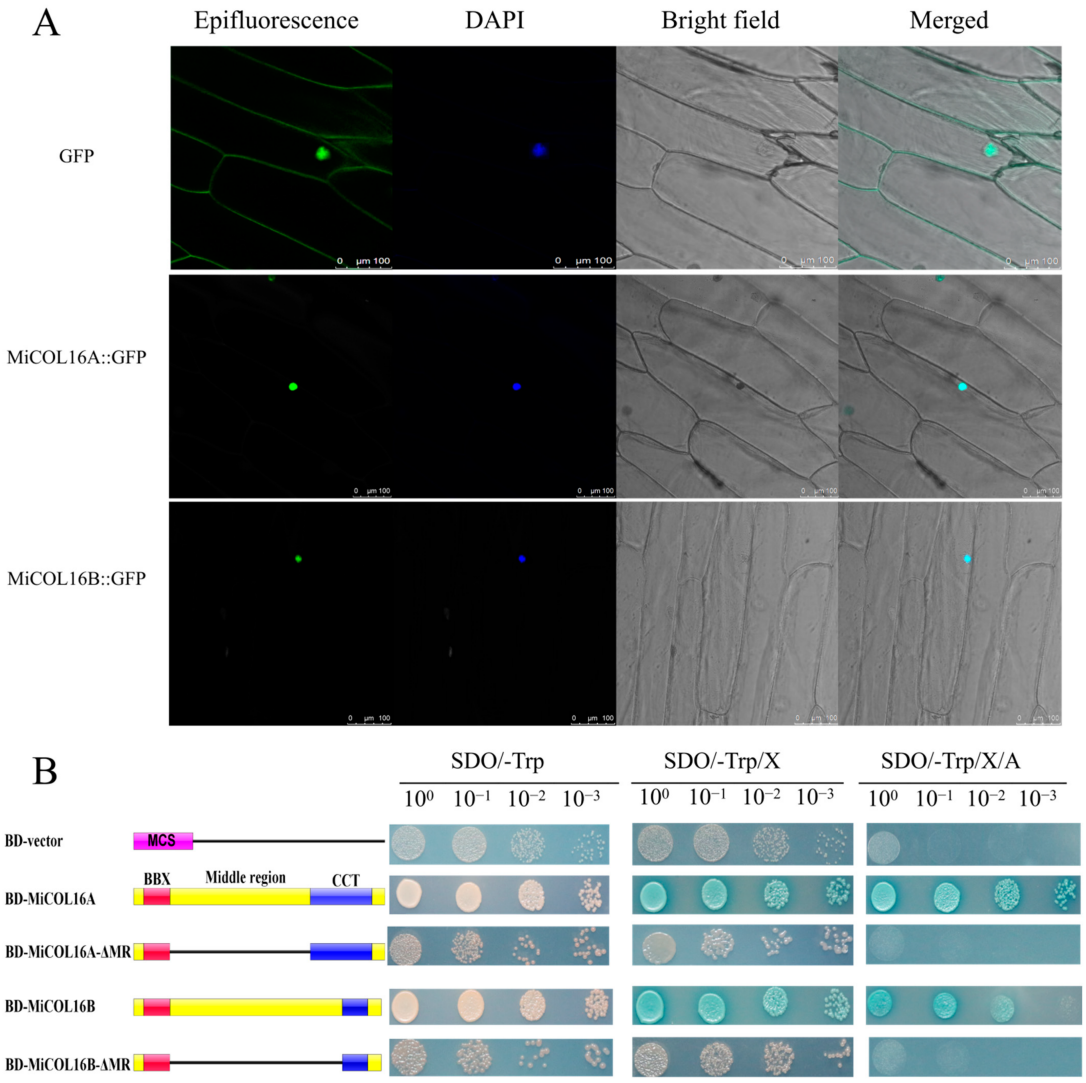

Figure 4. (**A**) Subcellular localization. Scale bars = 100 μm. (**B**) Transcriptional activation activity. The left diagram shows various constructs. MCS, multiple cloning sites; BD, GAL4-DNA binding domain; BBX, B-box; CCT, CO, CO-like, TOC1; MR, middle region.

A transcriptional activity assay was performed in yeast cells to demonstrate whether *MiCOL16A* or *MiCOL16B* had transcriptional activation activity. According to a previous study, the MR between the B-BOX and CCT domains is required for CO transcriptional activity [24][32][33]. Thus, *MiCOL16A, MiCOL16B, MiCOL16A*-ΔMR and MiCOL16B-ΔMR were fused into a pGBKT7 vector, and an empty pGBKT7 vector was used as a control. The five different plasmids were transferred into yeast cells, which were then transferred onto different plates. Three days later, all the transformants grew equally well on selective SD/-Trp media. On these three selective media, the BD-MiCOL16A and BD-MiCOL16B transformants grew well and turned blue, but the yeast transformed with the BD-vector, BD-MiCOL16A-ΔMR and BD-MiCOL16B-ΔMR grew only on SD/-Trp/X-α-gal plates and did not turn blue (**Figure 4**B). Together, α-gal activity could not be detected when the MR region was deleted. These results showed that through their MR domains, *MiCOL16A* and *MiCOL16B* have transcriptional activation activity in yeast.

5. Overexpression of MiCOL16A and MiCOL16B Delayed Flowering in Arabidopsis

To determine whether *MiCOL16A* and *MiCOL16B* are involved in the regulation of flowering time, they were overexpressed in *Arabidopsis* (under the control of the CaMV 35S promoter). Researchers obtained 15 and 10 independent transgenic lines of *MiCOL16A* and *MiCOL16B*, respectively, and researchers selected three homozygous lines for each construct from within the T3 generation and planted them under LD or SD conditions. The PCR analysis results showed that *MiCOL16A* and *MiCOL16B* were expressed in the transgenic plants but not in the WT or empty vector-transformed *Arabidopsis* plants under LD (**Figure 5**(A1,B1)) or SD conditions (**Figure 6**(A1,B1)). Under LD and SD conditions, both the *MiCOL16A* and *MiCOL16B* transgenic lines flowered later than the WT and empty vector-transformed plants. At flowering, compared with the WT and empty vector-transformed plants, the *MiCOL16A* and *MiCOL16B* transgenic plants had more rosette leaves (**Figure 5** and **Figure 6**) (**Table 1**).

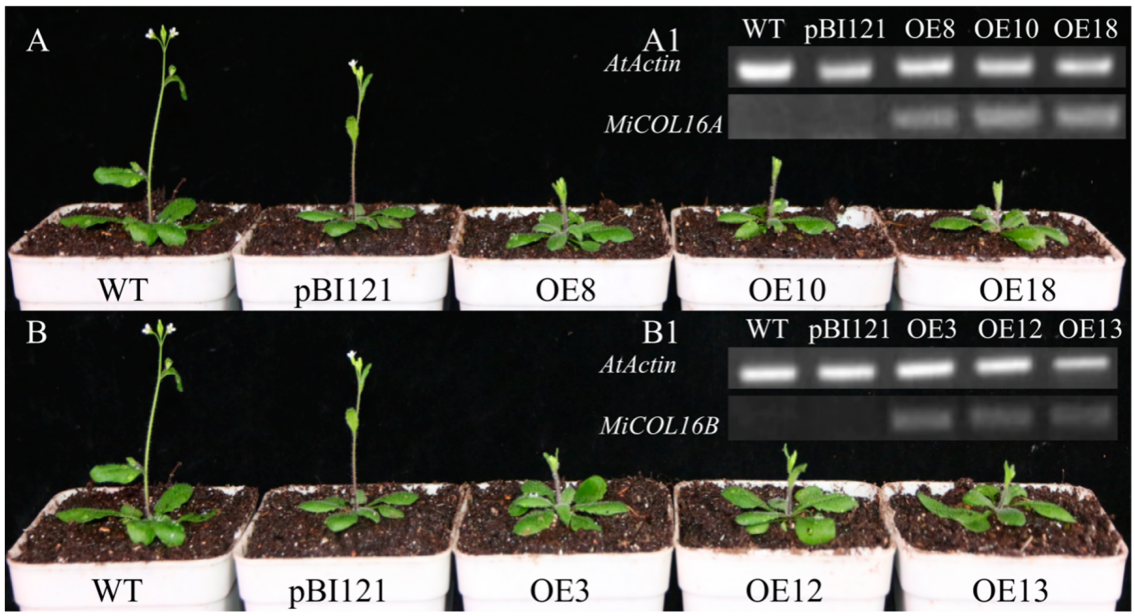

Figure 5. Ectopic expression of *MiCOL16A* and *MiCOL16B* delayed flowering under LD conditions. (**A1**,**B1**) Expression of *MiCOL16A* (**A1**) and *MiCOL16B* (**B1**) in the WT, empty vector-transformed and overexpression plants. (**A**) *MiCOL16A* transgenic *Arabidopsis* plants under LD conditions. (**B**) *MiCOL16B* transgenic *Arabidopsis* plants under LD conditions.

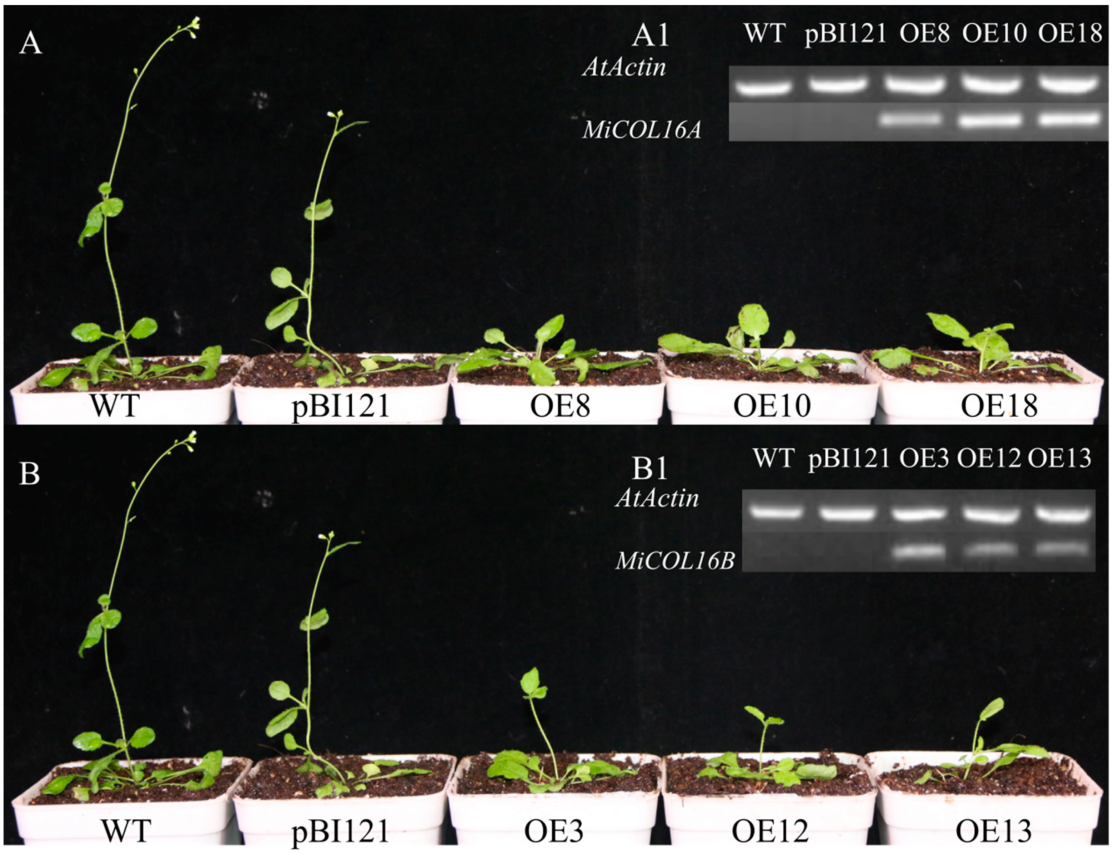

Figure 6. Ectopic expression of *MiCOL16A* and *MiCOL16B* delayed flowering under SD conditions. (**A1**,**B1**) Expression of *MiCOL16A* (**A1**) and *MiCOL16B* (**B1**) in the WT, empty vector-transformed and overexpression plants. (**A**) *MiCOL16A* transgenic *Arabidopsis* plants under SD conditions. (**B**) *MiCOL16B* transgenic *Arabidopsis* plants under SD conditions.

Table 1. Overexpression of *MiCOL16A* and *MiCOL16B* repressed flowering in *Arabidopsis*.

ID	Days to Flowering		No. Rosette Leaves		Plant Height [a] (cm)	
	LD	SD	LD	SD	LD	SD
WT	24.8 ± 0.6	50.1 ± 0.8	5.5 ± 0.5	7.2 ± 0.3	6.4 ± 0.8	11.4 ± 0.6
pBI121	25.6 ± 0.4	49.6 ± 0.7	7.6 ±0.6	7.0 ± 0.5	6.7 ± 0.4	11.7 ± 0.4
MiCOL16A						
OE2	28.0 ± 0.3 *	51.3 ± 0.8	6.3 ± 0.4	7.6 ± 0.3	4.6 ± 1.1 *	14.2 ± 0.9 *
OE8	28.0 ± 0.5 *	52.8 ± 0.2 *	6.8 ± 0.6 *	7.3 ± 0.7	4.5 ± 0.6 *	14.2 ± 0.8 *
OE10	28.1 ± 0.8 *	52.8 ± 0.3 *	7.5 ± 1.0 *	7.3 ± 0.5	6.2 ± 1.1	13.0 ± 0.3 *
MiCOL16B						
OE3	27.6 ± 0.5 *	53.0 ± 0.4 *	6.6 ± 0.7 *	7.4 ± 0.6	4.7 ± 1.0 *	17.7 ± 1.1 *

ID	Days to Flowering		No. Rosette Leaves		Plant Height [a] (cm)	
	LD	SD	LD	SD	LD	SD
OE12	26.9 ± 0.8 *	51.2 ± 0.9	7.1 ± 0.5 *	7.3 ± 0.4	5.2 ± 1.1 *	17.1 ± 1.0 *
OE13	28.4 ± 0.5 *	51.5 ± 0.4 *	6.7 ± 0.7 *	6.6 ± 0.6	4.3 ± 0.8 *	13.4 ± 0.2 *

[a] Plant height was measured at the time of flowering. Significant differences among the samples were assessed at the $p < 0.05$ (*) level by Student's *t* tests.

To further dissect the expression patterns of the floral integrator genes in the *MiCOL16A* and *MiCOL16B* overexpression lines, the transcript levels of *AtFT* and *AtSOC1* were measured in the WT and overexpression plants under LD or SD conditions (**Figure 7**). The results showed that both *MiCOL16A* and *MiCOL16B* significantly repressed the expression of *AtSOC1* and *AtFT* in *Arabidopsis* under LD and SD conditions.

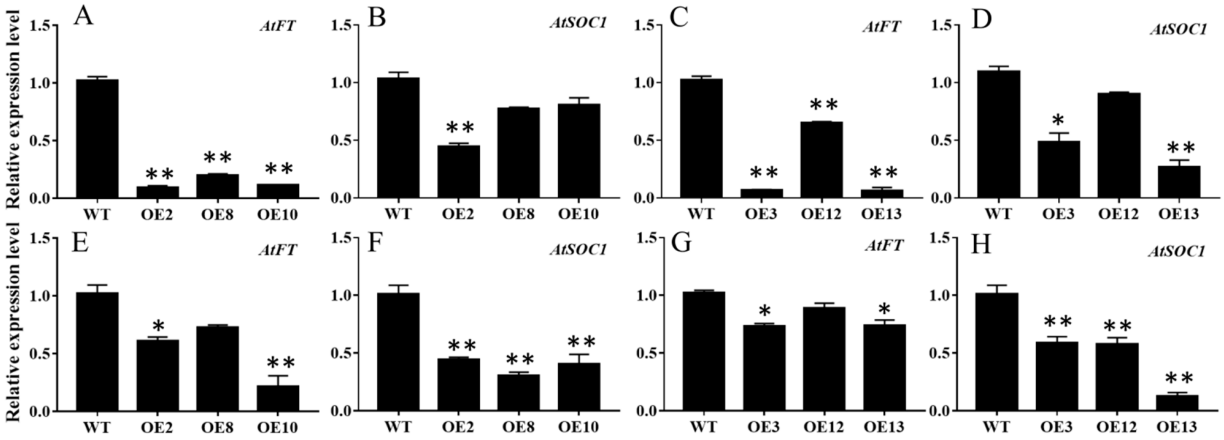

Figure 7. Expression patterns of flowering-related genes. (**A**–**D**) Expression patterns of *AtFT* and *AtSOC1* in the WT and the *MiCOL16A* (**A**,**B**) or *MiCOL16B* (**C**,**D**) overexpression plants under LD conditions. (**E**–**H**) Expression levels of *AtFT* and *AtSOC1* in the WT and the *MiCOL16A* (**E**,**F**) or *MiCOL16B* (**G**,**H**) overexpression plants under SD conditions. Significant differences among the samples were assessed at the $p < 0.05$ (*) and $p < 0.01$ (**) levels by Student's *t* tests.

6. MiCOL16A and MiCOL16B Enhance Tolerance to Abiotic Stress

To assess the effect of ectopic *MiCOL16A* and *MiCOL16B* expression in response to abiotic stress, three homozygous lines (T3 generation) were selected. Three-day-old seedlings of the overexpression and WT plants were transplanted onto half-strength MS media supplemented with mannitol and NaCl. The length of their roots was measured after 7 days of stress treatment. The untreated WT and overexpression plants did not significantly differ, but compared with the WT plants, both *MiCOL16A* and *MiCOL16B* overexpression plants grew better and had longer roots under all stress conditions (**Figure 8** and **Figure 9**). Together, these results showed that,

compared with WT plants, *MiCOL16A* and *MiCOL16B* transgenic plants had improved tolerance to drought and salt stress.

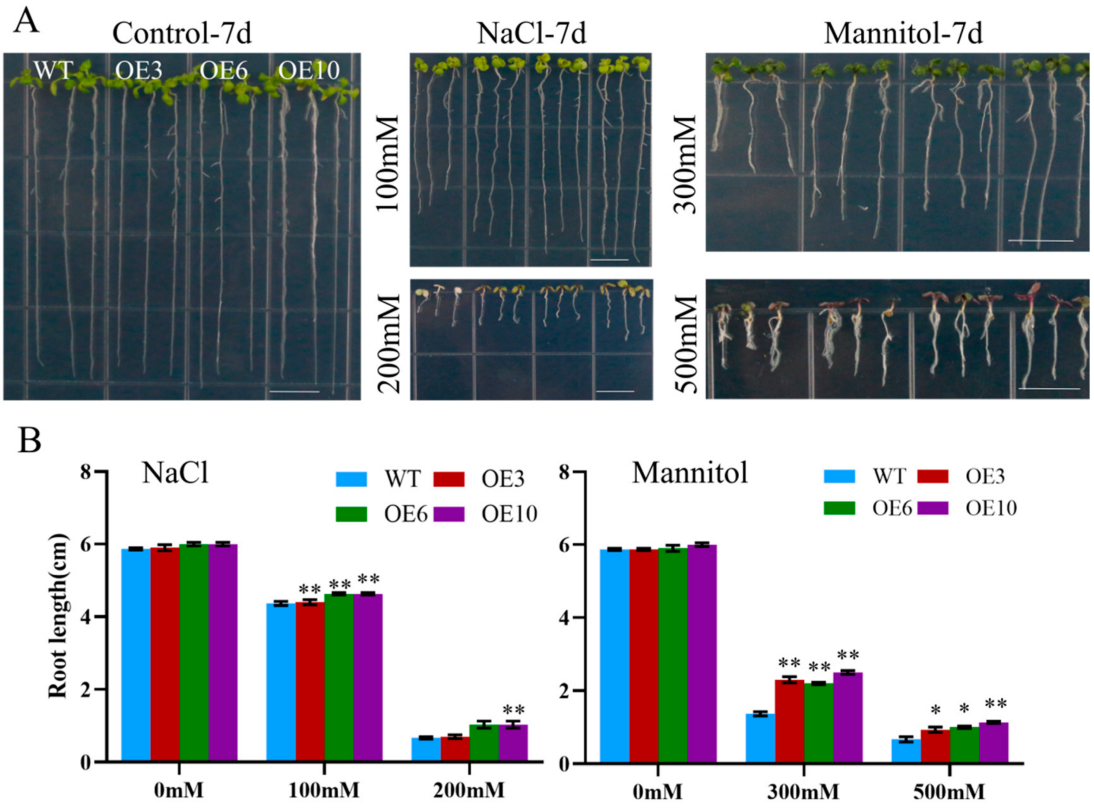

Figure 8. Assays of the length of the primary roots of WT and *MiCOL16A* transgenic lines under abiotic stress. (**A**) Seeds of the WT and three transgenic lines grown on half-strength MS media and subjected to various stresses. The bars represent 1.0 cm. (**B**) Lengths of the roots of all the lines under salt and drought treatment. Significant differences among the samples were assessed at the $p < 0.05$ (*) and $p < 0.01$ (**) levels by Student's *t* tests.

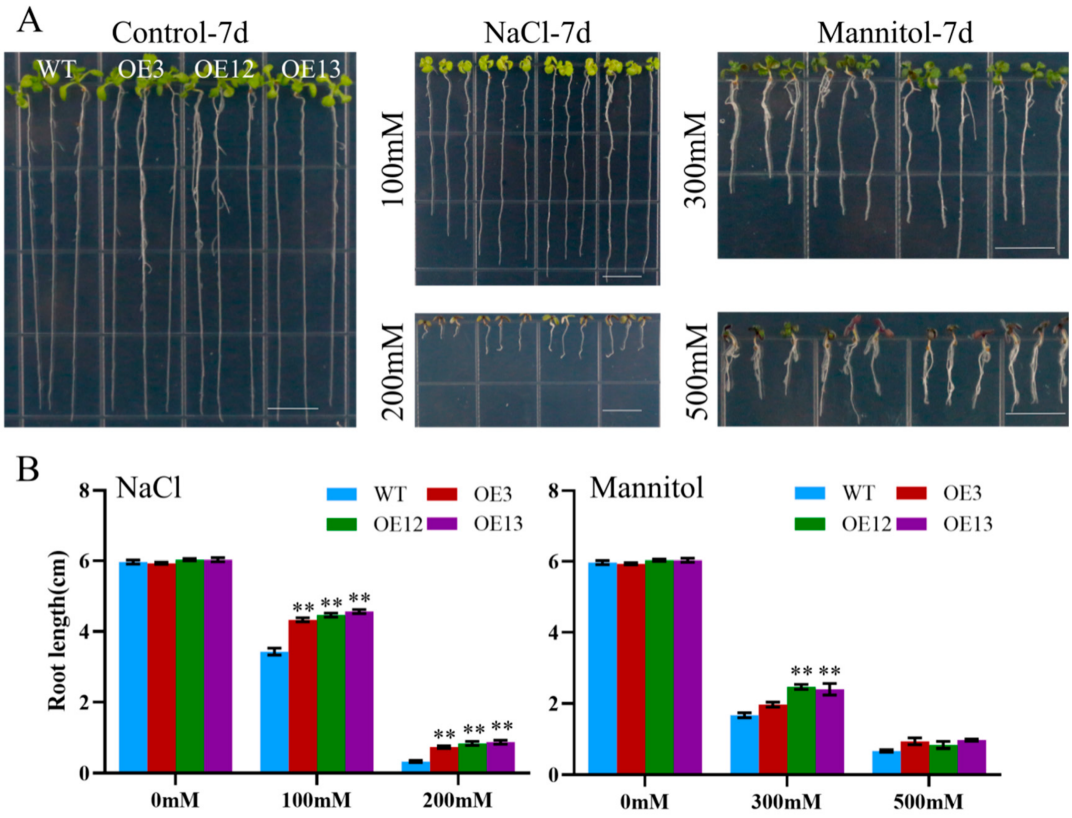

Figure 9. Assays of the length of the primary roots of the WT and *MiCOL16B* transgenic lines under abiotic stress. (**A**) Seeds of the WT and three transgenic lines grown on half-strength MS media and subjected to various stresses. The bars represent 1.0 cm. (**B**) Lengths of the roots of all the lines under salt and drought treatment. Significant differences among the samples were assessed at the $p < 0.01$ (**) levels by Student's *t* tests.

To further determine the response of *MiCOL16A* and *MiCOL16B* transgenic plants to abiotic stress, 7-day-old seedlings were transplanted into square pots. After the seedlings were allowed to recover, they were watered with 300 mM NaCl every 2 days, and regular water was withheld (**Figure 10**A,B). For salt treatment, the survival rate was measured when obvious phenotypic differences occurred. Approximately 20.0% of WT plants, 80.0% of *OEMiCOL16A*#3 plants, 93.3% of *OEMiCOL16A*#6 plants and 86.7% of *OEMiCOL16A*#10 plants survived (**Figure 10**C). Similarly, approximately 26.7% of WT plants survived, but 73.3% of *OEMiCOL16B*#3, 93.3% of *OEMiCOL16B*#12 and 86.7% of *OEMiCOL16B*#13 plants survived (**Figure 10**D). With respect to the drought treatment, the survival rate was measured after the plants had been rewatered for 3 days: a total of 6.7% of WT plants survived, but 93.3% of *OEMiCOL16A*#3, 80.0% of *OEMiCOL16A*#6 and 73.3% of *OEMiCOL16A*#10 plants survived (**Figure 10**C). Similarly, no WT survived, but 40.0% of *OEMiCOL16B*#3, 93.3% of *OEMiCOL16B*#12 and 80.0% of *OEMiCOL16B*#13 lines survived (**Figure 10**D). Together, these results showed that overexpression of *MiCOL16A* and *MiCOL16B* in *Arabidopsis* improved salt and drought tolerance.

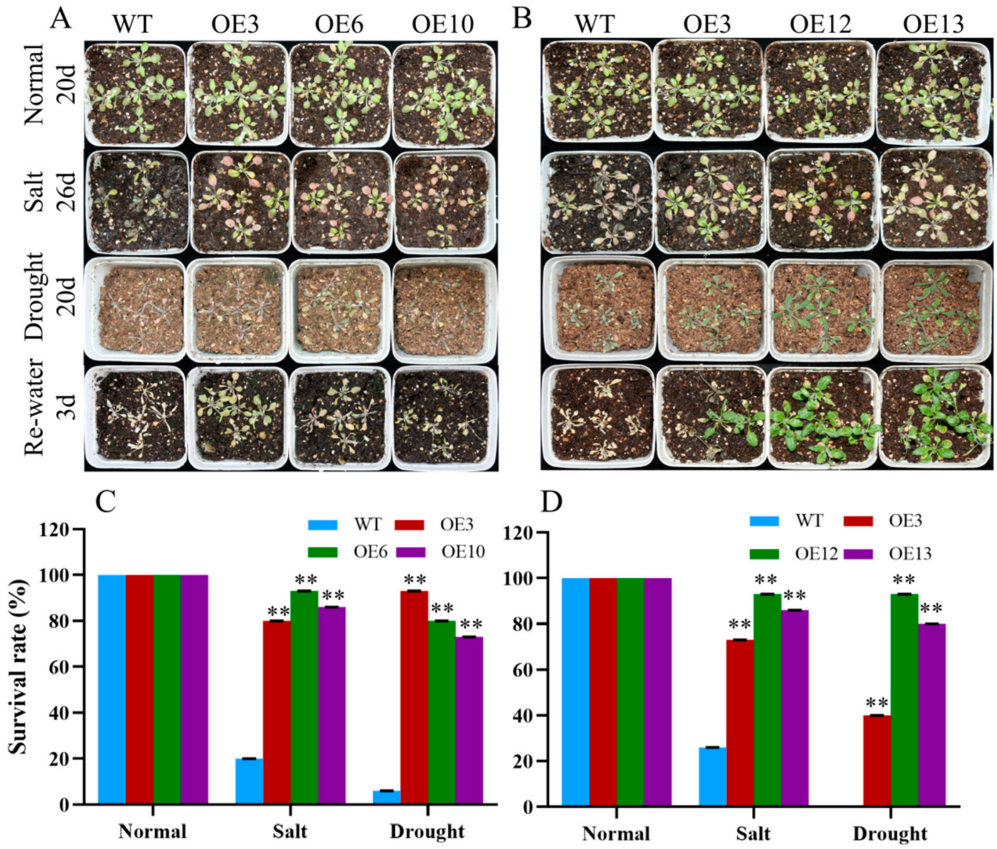

Figure 10. Phenotypes of WT and *MiCOL16A* and *MiCOL16B* transgenic plants under abiotic stresses. Normal, control; salt, 300 mM NaCl solution applied every 2 days; drought, withholding of water. (**A**) WT and *MiCOL16A* transgenic plants under different stresses. (**B**) WT and *MiCOL16B* transgenic lines under different stresses. (**C**–**D**) Survival rates of the WT and the *MiCOL16A* (**C**) and *MiCOL16B* (**D**) transgenic lines under different stresses. Significant differences among the samples were assessed at the $p < 0.01$ (**) levels by Student's *t* tests.

To explore the molecular mechanism underlying these phenomena in the transgenic lines in response to salt or drought, four stress-related genes were selected: *AtNHX1, AtRD20, AtSOS1* and *AtCOR15A* (**Figure 11**). Under salt stress, the expression levels of *AtNHX1, AtRD20* and *AtSOS1* were significantly higher in the three transgenic lines of *MiCOL16A* than in the WT, but in the *MiCOL16B* transgenic lines, the expression level of *AtRD20* was not significantly higher (**Figure 11**A,B). Under drought conditions, the expression levels of *AtCOR15A*, *AtRD20* and *AtNHX1* in the *MiCOL16A* and *MiCOL16B* transgenic lines were significantly higher than those in the WT (**Figure 11**C,D). These findings showed that by regulating the expression of stress-responsive genes, the *MiCOL16A* and *MiCOL16B* genes might increase the stress tolerance of transgenic plants under drought or salt stress.

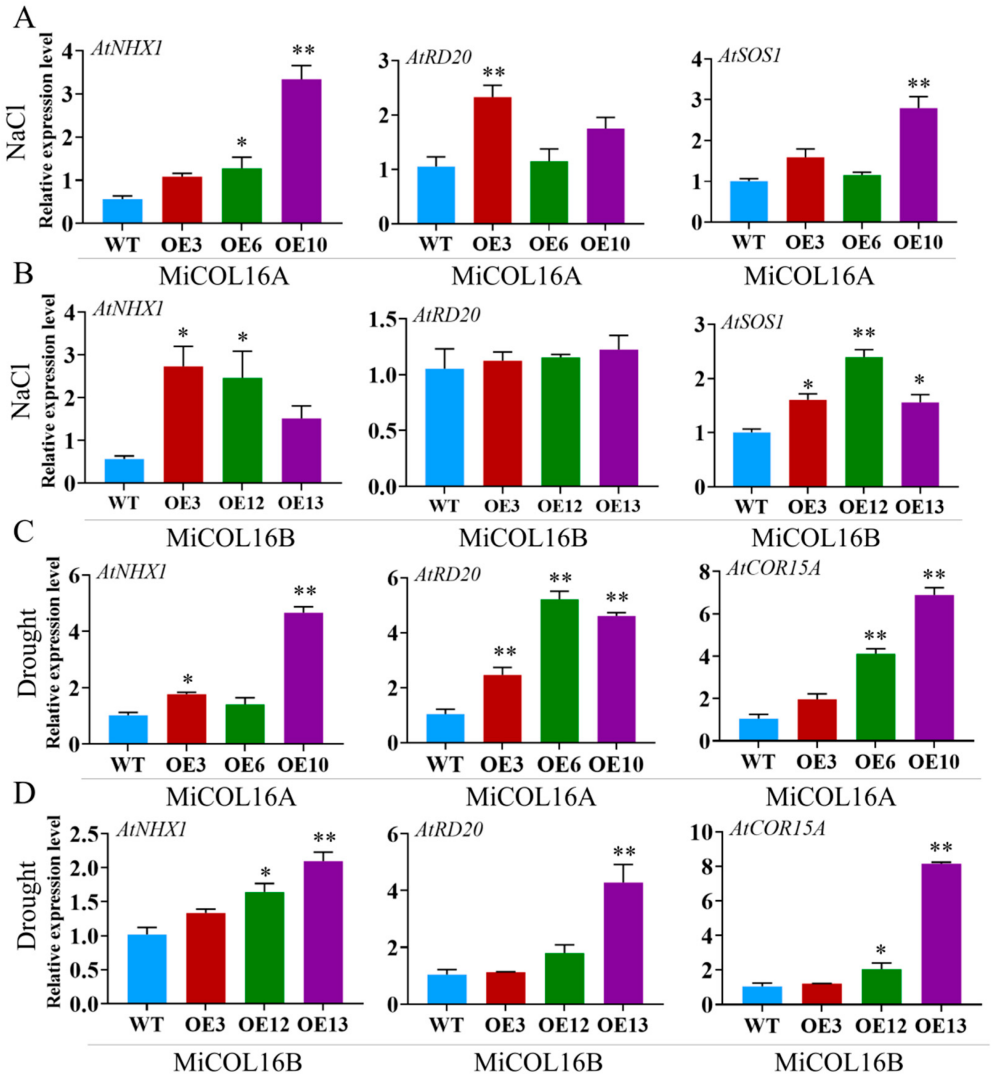

Figure 11. Expression patterns of stress-responsive genes in WT and *MiCOL16A* and *MiCOL16B* transgenic lines. (**A**,**B**) Salt stress conditions. Expression levels of the *AtNHX1*, *AtRD20* and *AtSOS1* genes in *MiCOL16A* (**A**) and *MiCOL16B* (**B**) transgenic lines. (**C**,**D**) Drought stress conditions. Expression levels of the *AtNHX1*, *AtRD20* and *AtCOR15A* genes in the *MiCOL16A* (**C**) and *MiCOL16B* (**D**) transgenic lines. Significant differences among the samples were assessed at the $p < 0.05$ (*) and $p < 0.01$ (**) levels by Student's *t* tests.

References

1. Okamuro, J.K.; Szeto, W.; Lotys-Prass, C.; Jofuku, K.D. Photo and hormonal control of meristem identity in the Arabidopsis flower mutants apetala2 and apetala1. Plant Cell 1997, 9, 37–47.
2. Wu, G.; Park, M.Y.; Conway, S.R.; Wang, J.W.; Weigel, D.; Poethig, R.S. The sequential action of miR156 and miR172 regulates developmental timing in Arabidopsis. Cell 2009, 138, 750–759.
3. Blazquez, M.A.; Green, R.; Nilsson, O.; Sussman, M.R.; Weigel, D. Gibberellins promote flowering of Arabidopsis by activating the LEAFY promoter. Plant Cell 1998, 10, 791–800.

4. Huang, G.W.; Ma, J.H.; Han, Y.Z.; Chen, X.J.; Fu, Y.F. Cloning and expression analysis of the soybean CO-like gene GmCOL9. Plant Mol. Biol. Rep. 2010, 29, 352–359.
5. Komeda, Y. Genetic regulation of time to flower in Arabidopsis thaliana. Annu. Rev. Plant Biol. 2004, 55, 521–553.
6. Putterill, J.; Robson, F.; Lee, K.; Simon, R.; Coupland, G. The CONSTANS gene of Arabidopsis promotes flowering and encodes a protein showing similarities to zinc finger transcription factors. Cell 1995, 80, 847–857.
7. Griffiths, S.; Dunford, R.P.; Coupland, G.; Laurie, D.A. The evolution of CONSTANS-like gene families in barley, rice, and Arabidopsis. Plant Physiol. 2003, 131, 1855–1867.
8. Yano, M.; Katayose, Y.; Ashikari, M.; Yamanouchi, U.; Monna, L.; Fuse, T.; Baba, T.; Yamamoto, K.; Umehara, Y.; Nagamura, Y.; et al. Hd1, a major photoperiod sensitivity quantitative trait locus in rice, is closely related to the Arabidopsis flowering time gene CONSTANS. Plant Cell 2000, 12, 2473–2484.
9. Serrano, G.; Herrera-Palau, R.; Romero, J.M.; Serrano, A.; Coupland, G.; Valverde, F. Chlamydomonas CONSTANS and the evolution of plant photoperiodic signaling. Curr. Biol. 2009, 19, 359–368.
10. Imaizumi, T.; Schultz, T.F.; Harmon, F.G.; Ho, L.A.; Kay, S.A. FKF1 F-box protein mediates cyclic degradation of a repressor of CONSTANS in Arabidopsis. Science 2005, 309, 293–297.
11. Sawa, M.; Nusinow, D.A.; Kay, S.A.; Imaizumi, T. FKF1 and GIGANTEA complex formation is required for day-length measurement in Arabidopsis. Science 2007, 318, 261–265.
12. Imaizumi, T.; Kay, S.A. Photoperiodic control of flowering: Not only by coincidence. Trends Plant Sci. 2006, 11, 550–558.
13. Wigge, P.A.; Kim, M.C.; Jaeger, K.E.; Busch, W.; Schmid, M.; Lohmann, J.U.; Weigel, D. Integration of spatial and temporal information during floral induction in Arabidopsis. Science 2005, 309, 1056–1059.
14. Shogo, I.; Young, H.S.; Anna, R.J.; Ryan, J.M.; Ghislain, B.; Richard, G.O.; Takato, I. FLOWERING BHLH transcriptional activators control expression of the photoperiodic flowering regulator CONSTANS in Arabidopsis. Proc. Natl. Acad. Sci. USA 2012, 109, 3582–3587.
15. Sun, J.J.; Lu, J.; Bai, M.J.; Chen, Y.Q.; Wang, W.N.; Fan, C.G.; Liu, J.Y.; Ning, G.G.; Wang, C.Q. Phytochrome-interacting factors interact with transcription factor CONSTANS to suppress flowering in rose. Plant Physiol. 2021, 186, 1186–1201.
16. Ana, L.; Federico, V.; Manuel, P.; Jose, A.J. The Arabidopsis E3 ubiquitin ligase HOS1 negatively regulates CONSTANS abundance in the photoperiodic control of flowering. Plant Cell 2012, 24, 982–999.

17. Liu, L.J.; Zhang, Y.C.; Li, Q.H.; Sang, Y.; Mao, J.; Lian, H.L.; Wang, L.; Yang, H.Q. COP1-Mediated ubiquitination of CONSTANS is implicated in cryptochrome regulation of flowering in Arabidopsis. Plant Cell 2008, 20, 292–306.
18. Yang, N.; Cong, Q.; Cheng, L.J. BBX transcriptional factors family in plants-a review. Chin. J. Biotechnol. 2019, 36, 666–677.
19. Ledger, S.; Strayer, C.; Ashton, F.; Kay, S.A.; Putterill, J. Analysis of the function of two circadian-regulated CONSTANS-LIKE genes. Plant J. 2001, 26, 15–22.
20. Graeff, M.; Straub, D.; Eguen, T.; Dolde, U.; Rodrigues, V.; Brandt, R.; Wenkel, S. Microprotein-mediated recruitment of CONSTANS into a topless trimeric complex represses flowering in Arabidopsis. PLoS Genet. 2016, 12, e1005959.
21. Wang, H.G.; Zhang, Z.L.; Li, H.Y.; Zhao, X.Y.; Liu, X.M.; Ortiz, M.; Lin, C.T.; Liu, B. CONSTANS-LIKE 7 regulates branching and shade avoidance response in Arabidopsis. J. Exp. Bot. 2013, 64, 1017–1024.
22. Takase, T.; Kakikubo, Y.; Nakasone, A.; Nishiyama, Y.; Yasuhara, M.; Yoko, T.; Kiyosue, T. Characterization and transgenic study of CONSTANS-LIKE8 (COL8) gene in Arabidopsis thaliana: Expression of 35S:COL8 delays flowering under long-day conditions. Plant Biotechnol. 2011, 28, 439–446.
23. Tsuji, H.; Taoka, K.; Shimamoto, K. Regulation of flowering in rice: Two florigen genes, a complex gene network, and natural variation. Curr. Opin. Plant Biol. 2011, 14, 45–52.
24. Wu, W.X.; Zheng, X.M.; Chen, D.B.; Zhang, Y.X.; Ma, W.W.; Zhang, H.; Sun, L.P.; Yang, Z.F.; Zhao, C.D.; Zhan, X.D.; et al. OsCOL16, encoding a CONSTANS-like protein, represses flowering by upregulating Ghd7 expression in rice. Plant Sci. 2017, 260, 60–69.
25. Gonzalez-Schain, N.D.; Dıaz-Mendoza, M.; Zurczak, M.; Suárez-López, P. Potato CONSTANS is involved in photoperiodic tuberization in a graft-transmissible manner. Plant J. 2012, 70, 678–690.
26. Jeong, D.H.; Sung, S.K.; An, G. Molecular cloning and characterization of CONSTANS-like cDNA clones of the Fuji apple. J Plant Biol. 1999, 42, 23–31.
27. Luo, C.; Yu, H.X.; Fan, Y.; Zhang, X.J.; He, X.H. Research advance on the flowering mechanism of mango. Acta Hortic. 2019, 1244, 2.
28. Fan, Z.Y.; He, X.H.; Fan, Y.; Yu, H.X.; Wang, Y.H.; Xie, X.J.; Liu, Y.; Mo, X.; Wang, J.Y.; Luo, C. Isolation and functional characterization of three MiFTs genes from mango. Plant Physiol. Biochem. 2020, 155, 169–176.
29. Wei, J.Y.; Liu, D.B.; Liu, G.Y.; Tang, J.; Chen, Y.Y. Molecular cloning, characterization, and expression of MiSOC1: A homolog of the flowering gene SUPPRESSOR OF overexpression OF CONSTANS1 from mango (Mangifera indica L). Front. Plant Sci. 2016, 7, 1758.

30. Yu, H.X.; Luo, C.; Fan, Y.; Zhang, X.J.; Huang, F.; Li, M.; He, X.H. Isolation and characterization of two APETALA1-Like genes from mango (Mangifera indica L.). Sci. Hortic. 2020, 259, 108814.
31. Liu, Y.; Luo, C.; Zhang, X.J.; Lu, X.X.; Yu, H.X.; Xie, X.J.; Fan, Z.Y.; Mo, X.; He, X.H. Overexpression of the mango MiCO gene delayed flowering time in transgenic Arabidopsis. Plant Cell Tissue Organ Cult. 2020, 143, 219–228.
32. Tan, J.J.; Jin, M.N.; Wang, J.C.; Wu, F.Q.; Sheng, P.K.; Cheng, Z.J.; Wang, J.L.; Zheng, X.M.; Chen, L.P.; Wang, M.; et al. OsCOL10, a CONSTANS-Like gene, functions as a flowering time repressor downstream of Ghd7 in rice. Plant Cell Physiol. 2016, 57, 798–812.
33. Wu, W.X.; Zhang, Y.X.; Zhang, M.; Zhan, X.D.; Shen, X.H.; Yu, P.; Chen, D.B.; Liu, Q.E.; Sinumporn, S.; Hussain, K.; et al. The rice CONSTANS-like protein OsCOL15 suppresses flowering by promoting Ghd7 and repressing RID1. Biochem. Biophys. Res. Commun. 2018, 495, 1349–1355.